Glacial sedimentation in Northern Gondwana: insights from the Talchir formation, Manendragarh, India

Adrita Choudhuri[1,*], Sabyasachi Mandal[1], Adam Bumby[2] and S. Suresh Kumar Pillai[1]

[1] Birbal Sahni Institute of Palaeosciences, Lucknow, India and

[2] Department of Geology, University of Pretoria, South Africa

*Corresponding author: Adrita Choudhuri; Email: adrita.choudhuri@bsip.res.in

Abstract

Among the vast swathes of Gondwanan sedimentary rocks in India, exposures of the Lower Permian Talchir Formation at Manendragarh in India are exceptional for their cold marine faunal assemblage and muddy conglomerates of possible glacial origin. They may represent a record of the late Palaeozoic glaciation that affected Gondwana in the Permo-Carboniferous. Although the fossil record is relatively well documented, the sedimentology of this area is not well understood. This paper intends to fill the gap in knowledge regarding palaeogeography and the palaeoenvironmental changes within the basin through space and time. We distinguish conglomerates that are formed by glacial and mass flow processes. The lateral variation in facies associations along a NNE-SSW transect in the study area identifies the depositional basin as an interior sea that formed when the sea spilled over a steep basement ridge during a transgression. The benthic organisms remained confined to the seaward basin margin where they only flourished in the initial stage of basin filling. Locally derived, bioclastic storm beds are limited to the seaward flank of the basin. Alternating phases of glaciation and interglaciation resulted in an interbedded succession of grey shales and interglacial density flow deposits. The channels that fed these density flows are preserved closest to the landward margin of the basin. Co-existence of glacial diamictites and interglacial density flow deposits highlights the climatic changes in this part of Gondwana during the Late Palaeozoic.

Keywords: Density flows; diamictites; Early Permian; glacial conglomerates; Palaeogeography

1. Introduction

Amidst the vast areal coverage of the Gondwanan rocks preserved in India, the Early Permian Talchir Formation at Manendragarh is exposed over a short 2.5 km stretch and is the only site in India where marine fossils are found. The fauna, which includes cold water varieties in association with muddy conglomerates, is claimed to be linked to the Gondwana glaciation in the Southern Hemisphere (Shah & Shastry, 1975; Dickins & Shah, 1979). Presently, the Indian government is developing the area as a geological museum to preserve this fossil suite, which is exceptional in an Indian context (Sinor, 1923; Reed, 1928; Ghosh, 1954; Bhatia & Saxena, 1957; Dutta, 1957; Tiwari, 1958; Bhatia & Singh, 1959; Bharti & Chakraborty, 2014). Although the fossil assemblage includes equivalents of those found in glacial Gondwana deposits on other continents, conclusive glacial features have not been reported from this locality. Muddy

conglomerates are present, but they could simply be nonglacial mass flow deposits (Dietrich *et al.* 2019). Paradoxically, deposits of mudflows or debris flows often coexist with deposits enriched in glacial dropstones (Chiarle *et al.* 2007; Tiranti & Deangeli, 2015; Vesely *et al.* 2018; Le Heron *et al.* 2022). A convincing explanation for the presence of marine black shale directly overlying the granitic basement is still absent. This field-based work aims to account for the sudden and dramatic change in hydraulic conditions implied by this unusual stratigraphic relationship (marine black shale onlapping the granite basement) and to reconstruct the variation in palaeogeography of the basin in tandem with the palaeoenvironment and depositional dynamics. We distinguish between sedimentary features that are of direct glacial origin and those that are more likely formed due to density flows.

2. Late Palaeozoic glaciation in Gondwana

Late Palaeozoic glaciation was conceived traditionally as a single and massive ice sheet covering all of southern Gondwana for duration of 100 million years (cf. Veevers & Powell, 1987; Frakes & Francis, 1988; Frakes *et al.* 1992; Ziegler *et al.* 1997; Hyde *et al.* 1999; Blakey, 2008; Buggisch *et al.* 2011). Glaciation started in western South America during the Visean (Caputo *et al.* 2008; Pérez Loinaze *et al.*, 2010) and ended in eastern Australia during the Middle to earliest Late Permian (Fielding *et al.* 2008a, 2008b, 2008c; Fielding *et al.* 2022). However, recent geochemical, isotopic age and biostratigraphic analyses have confirmed that the Late Palaeozoic glaciation was not continuous; rather, multiple smaller ice centres were activated at different times and places across Gondwana (Isbell *et al.* 2003, 2012; Fielding *et al.* 2008a, 2008d). A recent study also confirmed that, instead of a continuous 100 million-year span of glaciation, it was characterized by repeated short-lived glacial epochs (P1-P4, each spanning ~1–8 million years) separated by several ice-free intervals of similar duration (Montañez & Poulson, 2013 and references therein; Frank *et al.* 2015 and references therein; Griffis *et al.* 2021). Among these short-lived glacial phases, P1 (from Asselian to early Sakmarian) and P2 (from latest Sakmarian to early Artinskian) were the most intense, reaching their maxima and widespread distribution of ice sheets in Antarctica, eastern South America, Patagonia, Africa, the Arabian Peninsula, India, Australia, and some southern Asian crustal blocks (Isbell *et al.* 2003, 2011; Fielding *et al.* 2008a; Wopfner & Jin, 2009; Taboada, 2010; Frank *et al.* 2015 and references therein). However, the P3-P4 glacial phases were less intense, with small ice centres restricted only to Australia (Fielding *et al.* 2008a, 2008c, 2008d; Frank *et al.* 2015 and references therein). A recent study by Griffis *et al.* (2021) proposed that the glacial maximum of the Late Palaeozoic Icehouse was reached during the Carboniferous, not in the Permian. The warmer ice-free periods between glacial phases vary by location within Gondwana, being estuarine at times but also fluvial, open-marine, fossiliferous shallow marine facies, or a variety of other environments (Rogala *et al.* 2007; Fielding *et al.* 2008b; James *et al.* 2009; Fielding *et al.* 2010). The extensive glaciomarine deposits of the latest Pennsylvanian to Early Permian age (Fielding *et al.* 2008d) indicate that both glaciers and ice sheets in southern Gondwana reached sea level, requiring widespread cooling (Isbell et al. 2012).

2.a. Records of Late Palaeozoic glaciation in India

In India, Talchir sedimentary rocks (Late Carboniferous to Early Permian) deposited within fault-controlled half-graben-type basins along palaeosuture lineaments such as the Damodar Valley, Son-Mahanadi Basin and Satpura Basin (Banerjee *et al.* 2020) bear diagnostic glaciogenic signatures (e.g. dropstones, glacial till deposits, glacial pavement, repeated glacial advance-retreat cycles with shifts in the palaeoshorelines during the Talchir sedimentation) related to Late Palaeozoic glaciation (Smith, 1963a, 1963b; Casshyap & Qidwai, 1974; Das & Sen, 1980; Casshyap & Tewari, 1982; Eyles & McCabe, 1989; Bose *et al.* 1992; Mukhopadhyay & Bhattacharya, 1994; Veevers & Tewari, 1995; Bhattacharya *et al.* 2004, 2005; Maejima *et al.* 2004; Bhattacharya & Bhattacharya, 2006, 2010, 2012; Chakraborty & Ghosh, 2008 Varshney & Bhattacharya, 2023). A marine embayment within central India during the Early Permian was inferred based on the occurrence of marine invertebrates such as bivalves, brachiopods, gastropods, polyplacophora, crinoids, bryozoans, foraminifers, ostracods, among other invertebrates at Umaria and Manendragarh, and Dudhi Nala (Bhatia & Singh, 1959; Ghosh, 2003; Bharti &Chakraborty, 2014). Till deposits relating to at least three phases of Glacial advance and retreat during Talchir sedimentation are recorded in different sub-basins of the Damodar Valley (Smith, 1963a, 1963b; Sen, 1977, 1991). Trace fossil studies, cyclicity assessments and sequence stratigraphic architecture across different sub-basins of the Damodar Valley and the Satpura Basin revealed that storm-tide-influenced shallow marine deposition took place over these basal Talchir glaciogenic sediments due to alternating glacial advance-retreat phases (Bhattacharya, 2013; Bhattacharya & Bhattacharya, 2015) and are correlated with the climatic changes at the end of P1–P2 phases of Late Palaeozoic glaciation (Bhattacharya, 2013; Bhattacharya & Bhattacharya, 2015; Varshney & Bhattacharya, 2023). Based on the palaeontological evidence, the Manendragarh glacier was correlated to the late stage of the P1 phase of Late Palaeozoic glaciation by Shah and Shastry (1975) and Dickins and Shah (1979). Our detailed sedimentary facies analysis in Manendragarh once again reflects such short-term climatic transitions at the end of the P1 phase of Late Palaeozoic glaciation.

2.b. Geological background of the study area

The dominantly siliciclastic Talchir Formation is exposed on the banks of the River Hasdeo in Manendragarh, Surguja district, Chhattisgarh, central India, and was deposited in the Rewa sub-basin of the NW-SE-oriented Son-Mahanadi Basin (Fig. 1a; Mukherjee *et al.* 2012; Ram-Awatar *et al.* 2013; Acharya, 2018). Similar to all other Gondwanan basins of Peninsular India, the Rewa Sub-basin is a fault-controlled half-graben-type basin along a NW-SE-oriented palaeosuture of the Son-Mahanadi Basin (Fig. 1a; Acharya, 2018; Banerjee *et al.* 2020; Dasgupta, 2021). In the north, the Malwa Ridge separates the Rewa Sub-basin from the Son Basin (left side of the Malwa Ridge shown in Fig. 1a) and from the Mahanadi Graben in the south, bounded by two ridges, named the Manendragarh-Pratapur Ridge and the Naughata Ridge (Fig. 1a; Mukherjee *et al.* 2012; Dasgupta, 2021). There is substantial evidence in favour of glacially influenced sedimentation (e.g. dropstones, glacial till deposits, glacial pavement) throughout the Talchir Formation. (Pascoe, 1968; Mukhopadhyay *et al.* 2010; Varshney & Bhattacharya, 2023). Marine fossil assemblages have been recorded from several basins in

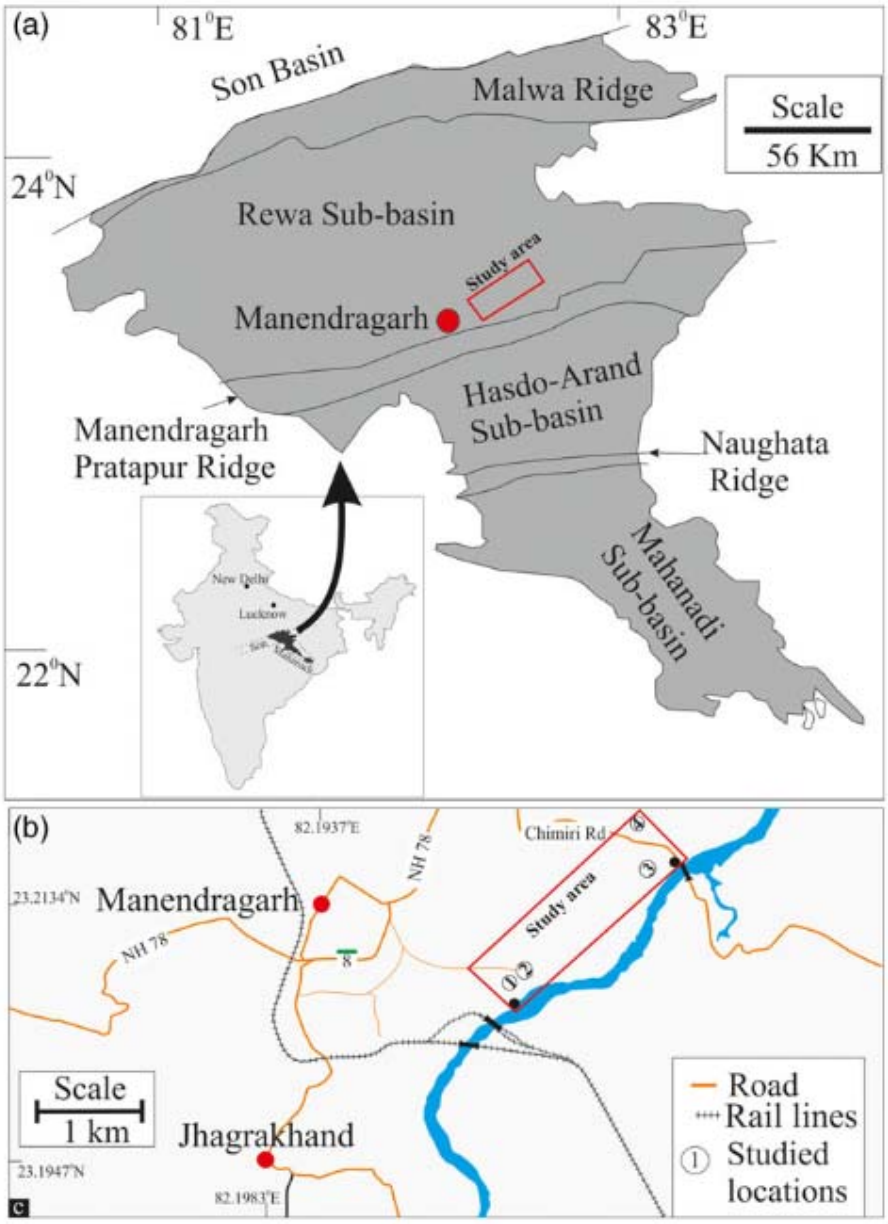

Figure 1. (a) Location of Manendragarh and the study area within the Rewa Sub-basin in the framework of related tectonic elements (map of India within inset). (b) Geographic location of the studied sections (1, 2, 3, 4) around Manendragarh.

Peninsular India where the Talchir Formation crops out, as well as along the Tethyan margin (Venkatachala & Tiwari, 1987; Ghosh, 2003; Mukhopadhyay *et al.* 2010; Bharti & Chakraborty, 2014; Mondal *et al.* 2021). However, supposedly glacial sediments and Early Permian marine fossils together occur nowhere in India except in the study area near Manendragarh (Bose *et al.* 1992; 1997; Chakraborty, 1993; Mukhopadhyay & Bhattacharya, 1994; Bhattacharya *et al.* 2004; Bhattacharya & Bhattacharya, 2015; Varshney & Bhattacharya, 2023). The faunal assemblage of Manendragarh includes Eurydesma, *Deltopecten* and *Trigonotreta hesdodoensis*, in addition to bryozoans, crinoids and foraminifers (Frakes *et al.* 1975; Dickins

& Shah, 1979; Venkatachala & Tiwari, 1987; Chandra, 1996). The fossil assemblages found in the studied locations have strong similarities with fossils found in other Gondwana basins in western Australia, Brazil, the Falkland Islands, Oman and South Africa (Table 1; Ghosh 2003; Fielding *et al.* 2006; Stephenson *et al.* 2007; Taboada *et al.* 2016; Horan *et al.* 2019; Simoes *et al.* 2020). Sahni and Dutt (1959) characterized its brachiopod assemblage by *Trigonotreta hesdodoensis*. A shallow marine origin of the Manendragarh fossils has been argued by many (e.g. Ghosh, 2003; Ram-Awatar *et al.* 2013; Table 1). The above-mentioned fauna found in the studied region are of cold water origin (Shen *et al.* 2013). Thus, the Manendragarh marine fossil-bearing beds of the Talchir deposits were correlated with the Late Carboniferous (Uralian) glaciation that continued up to the Early Permian (Artinskian) (Bhatia & Singh, 1959; Varshney & Bhattacharya, 2023). However, based on the marine fossils found in this studied area Shah and Shastry (1975) and Ram-Awatar *et al.* (2013) designated the marine fossil beds of the Talchir deposits as Early Permian age (280–240 Ma).

The patch of fossiliferous conglomerate beds is observed to be persistent along a ~2.5 km stretch of the NW bank of the Hasdeo River (Fig. 1b). The nonconformable contact of the Talchir deposits with the underlying Precambrian granite is characterized by basal Talchir strata deposited in graben structures developed in the granite (Acharya, 2018; Dasgupta, 2021). The Talchir Formation is overlain by the fluvial Barakar Formation (Casshyap & Tewari, 1984; Mukhopadhyay *et al.* 2010; Ram-Awatar *et al.* 2013).

Table 1. Marine fossils of Manendragarh, India and their equivalents in other continents described by previous workers

Fossil assemblage in Manendragarh		Equivalent fossil assemblage found in other continents	Palaeogeography interpreted based on the fossils	Climate/sea water temperature based on fossils
	E. Playfordi (Dickins, 1957)	Daltonganj and Rajhara, India (Ghosh, 2003)	Marine	—
	Eurydesma mytiloides (Reed, 1932)	Umaria, India (Ghosh, 2003)	Marine	—
	Eurydesma Sp.	Satpura, India (Ghosh, 2003)	Marine	—
		Sauce Grande Basin of eastern Argentina; and southern Sydney Basin, eastern Australia (Ivany & Runnegar, 2010; Cisterna *et al.* 2019; Garbelli *et al.* 2019)	Marine	Glaciation-deglaciation (Cisterna *et al.* 2019)/glacial-interglaciations (Garbelli *et al.* 2019)/1°c to 12°c (Ivany & Runnegar, 2010)
		Southern Sydney Basin, Australia (Fielding *et al.* 2006)	Shallow marine	
		Paraná Basin, Brazil (Taboada *et al.* 2016; Simões *et al.* 2020)	Marine	Glaciation-deglaciation
	Myonia? Sp.	SW Australia (Beard *et al.* 2015)	Marine	5°c to 12°c
	Eurydesma?cordatum; *Eurydesma? Globosum*; *Aviculopecten sp.*; *Pleurotomaria nuda* (Bhatia & Singh, 1959)	Salt Range; Kashmir, India; Australia; South Africa (Bhatia & Singh, 1959)	Marine	—
Brachiopod	*Trigonotreta hesdoensis* (Sahni & Dutt, 1959)	—	—	—

3. Palaeogeographic and palaeoenvironmental reconstruction

Palaeogeographic and palaeoenvironmental reconstruction is achieved through a comprehensive facies analysis. The Talchir Formation at Manendragarh is dominated by shale, the colour of which varies from black to grey. Conglomerates alternate with shale but

are not ubiquitous. Sandstones are minor components, associated with grey shale and their geometry varies spatially. Fossils are localized, although their hosting black shale is preserved extensively throughout the study area. Granite fragments embedded within the black shale range in size from boulders to small pebbles and their roundness varies from sharply angular to well-rounded.

Four different facies associations have been recognized in four different sections placed in a NE-SW, 2.5 km long transect bounded by outcrops of basement granite at both ends (Figs. 1b, 2). Each section displays a single facies association. All these four facies associations correspond to the lateral transition of each other, and do not represent vertical stacking (Fig. 2). We focus on facies associations (described below) instead of individual facies to interpret the depositional environment and ultimately the palaeogeographic framework. The same lithology may be shared between the associations, the latter differing significantly in a combination of lithic and biotic components, and bed geometry, structure and texture. Also, more importantly, all four studied sections directly/nonconformably overlie the granitic basement (Fig. 2; Acharya, 2018; Dasgupta, 2021). It highlights that all four facies associations are likely to be the result of lateral facies variation due to change in sea level and decreasing effects of glaciogenic processes. The facies associations are described below separately before presenting a general interpretation.

3.a. Facies Association I

This facies association is at the southern end of the transect and directly overlies the granitic basement (Fig. 2). Lithologically, it consists of two sub-facies viz. the shale (facies IA) and the calcarenite (facies IB). Facies IA is black, finely laminated (Fig. 3a, b) and is confined to the basal 2 m of the measured succession and contains granite fragments (Fig. 3b), which are similar in composition to that of the basement. Around the granite blocks, however, the laminae of the facies IA are obliterated (Fig. 3a). Some of the granite fragments are very large (>80 cm), irregular in shape and sharply angular (Fig. 3a). Facies IA also incorporates intact fossils (Fig. 3c), which include brachiopods and pelecypods, many of which are benthic, intact and occur dominantly in live positions (Fig. 3c). Towards the upper part of the section, facies IA gradually becomes fossil-free. In contrast to facies 1A, facies IB is lighter than facies IA, appears approximately 1 m above the base of the section, and then alternates upwards with facies IA (Fig. 3d). Facies IB is cross-stratified, approximately 20 cm thick, tabular in geometry and rich in broken shell fragments. Facies IB has sharp erosional and dented bases that are studded with black mud clasts (Fig. 3d, e). Locally, straight-crested ripples mantle the upper surface of the calcarenite beds (Fig. 3f). The ripples have a wavelength and amplitude of approximately 7.5 and 2 cm respectively. The thickness of the shale encased by successive calcarenite beds varies from 50–60 cm.

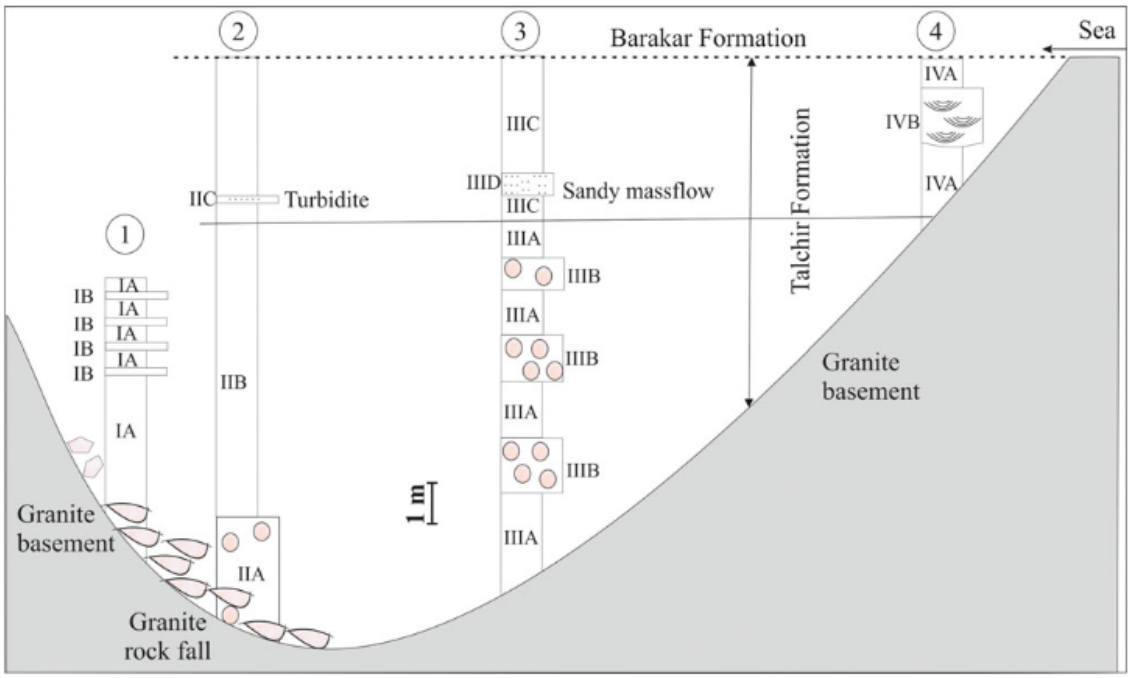

Figure 2. Schematic distribution of facies across the depositional basin.

3.a.1 Interpretation

The black shale (facies IA) and its marine invertebrate fossil content (Fig. 3c) bear a clear signature of its marine origin. Being deposited directly on top of the granite basement, facies IA bears a clear indication of rapid marine invasion, and a rapid rise in sea

level. Fine lamination within facies IA further points to a slow rate of deposition (Fig. 3a, b) and suggests that deposition took place in a stagnant basin where circulation was restricted (Posamentier & Walker, 2006). The invertebrate fossil content is restricted to the base of the formation and the southern end of the studied transect. Even the calcarenite beds (facies IB), rich in fossil debris, are also confined to Facies Association I in the southernmost part of the studied transect. It implies that the organisms could not thrive along the entire studied transect of Fig. 2. This could indicate that sediment accumulated under restricted circulation behind a basement ridge within a horst-graben structure (Fig. 2; Acharya, 2018; Dasgupta, 2021). The deposition is thus assumed to have taken place in an interior sea that formed when the sea spilled over the ridge during transgression. The presence of isolated large, Figure 1. (a) Location of Manendragarh and the study area within the Rewa Sub-basin in the framework of related tectonic elements (map of India within inset). (b) Geographic location of the studied sections (1, 2, 3, 4) around Manendragarh. angular granite boulders in Facies Association I (Fig. 3a, b) suggests that the basement ridge had been steep and was generated at the basin margin only. Hence, the seaward boundary on the southern side can be assumed to be steep.

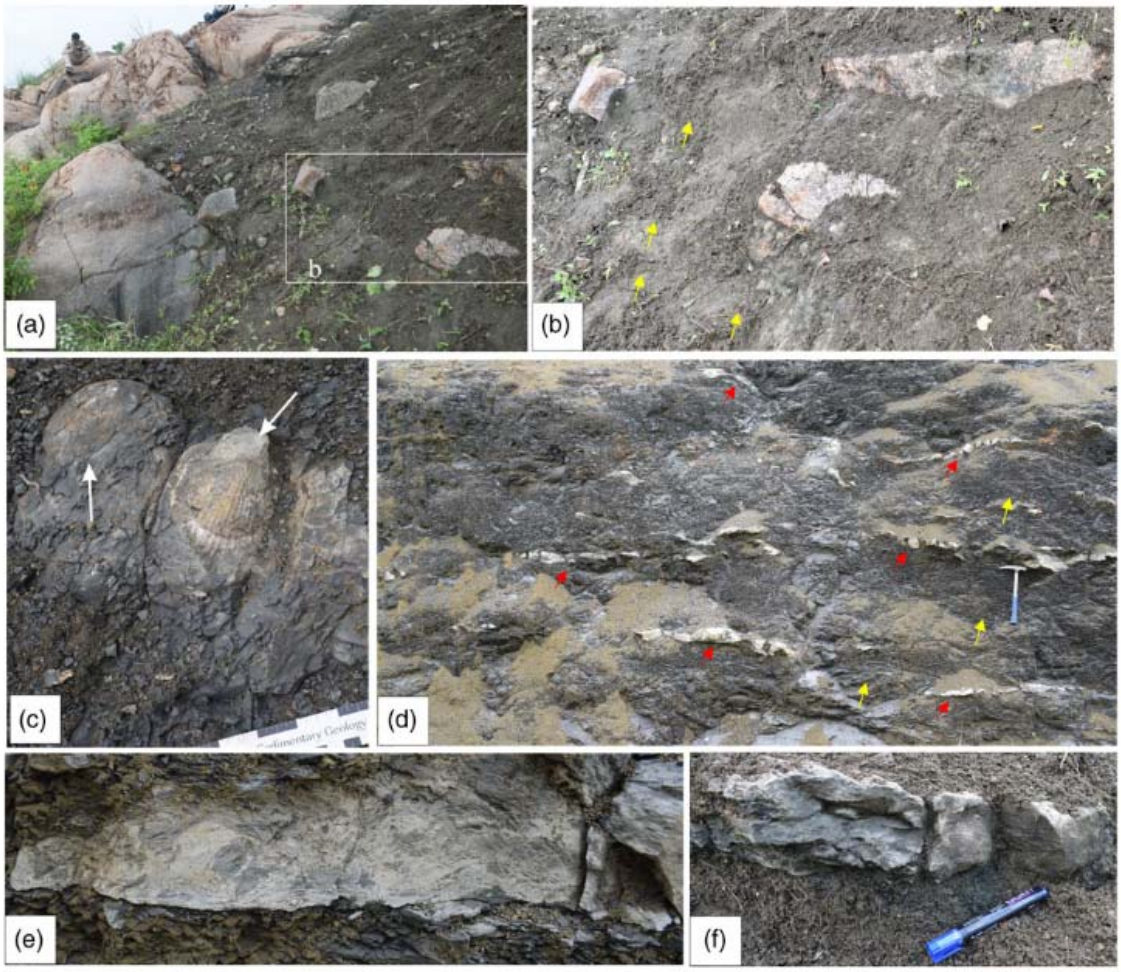

Figure 3. Facies Association I - (a) Granite ridge flanking black shale facies (IA) with scattered granite blocks of very widely variable diameter, sharp angularity and devoid of any arrangement in distribution. (b) Fine laminations (yellow arrows) preserved within black shale facies (IA). (c) Fossils present in live positions (arrowed) within black shale (IA) and calcarenite (IB) beds. (d) Alternations between the black shale (IA) and calcarenite beds (IB; arrowed). (e) Sharp and erosional base of the calcarenite bed (IB); note the black shale clasts present within the facies IB. (f) Wave ripple laminations on top of a calcarenite bed (IB).

Contrary to this concentration of marine fossils and unabraded granite boulders within Facies Association I at the southern boundary, the abraded granite pebbles increase in concentration rapidly from Facies Associations II to III, suggesting the existence of land northwards. This indicates that although there was input from both sides, the southern side provided large angular boulders from the steep basin margin whilst the northern side provided the conglomerates of cohesive/hyper-concentrated flow origin (discussed later).

The calcarenite facies (facies IB) is made of fragmented shells and is bound by facies IA below and above and appears to be a tempestite. Having a strongly erosional base and a wave-rippled top, these beds are interpreted as storm deposits, although the cross-strata within the beds could not be reconstructed clearly. The wave ripples on top of this likely tempestite record the waning phase of intermittent storms that eventually interrupted the usual calm depositional environment registered by the black shales above and below (Posamentier & Walker, 2006). The tempestite beds could have been emplaced by storm washovers spilling

over the basement ridge. As the sheet-like geometry was determined only at the outcrop scale and these beds were not found in other sections, they may be lenticular on a larger scale. This also implies that sea spilled over from the southern side of the ridge. The biotic colonies associated with the preserved shell fragments thus seem to have grown only on the seaward/southern flank of the depositional basin. It is apparent that the organisms had only limited success in colonizing the niche created immediately after the transgression; they were probably merely opportunistic. The cold temperature enhanced oxygen dissolution in the water column and, had there been ice sheets, glacial debris may have provided additional nutrients (Christ & Wernil Sr., 2014). The presence of the calcarenite facies (facies IB) at the site of Facies Association I alone suggests that only the distal fringe of the storm sheets is preserved.

3.b. Facies Association II

This facies association was found ~200 m away from outcrops of Facies Association I along the chosen transect (Fig. 2). It has three sub-facies viz. black shale (facies IIA), grey shale (facies IIB) and thin, sparse sandstone beds (facies IIC). Facies IIA occurs in the basal ~1 m and shares the same basal fossil assemblage (Fig. 4a) that is present within facies IA but the difference is that fossils are preserved as disarticulated valves in facies IIA (Fig. 4a). Unlike Facies Association I, the thickness of the fossiliferous zone of the facies IIA is reduced to 30 cm. Besides this, facies IIA also differs from the previously described facies IA in terms of the coexistence of scattered, well-rounded, small (approximately 16 cm in diameter) granite pebbles of the same composition (Fig. 4b). The thickness of this pebbly zone exceeds that of the fossiliferous zone, extending up to ~50 cm from the base of the section. Facies IIA however continues up to 1 m from the base of the section. The calcarenite beds noted in Facies Association I are notably absent in Facies Association II. The upper part of the section, approximately 2.5 m thick, is composed of grey shale (facies IIB; Fig. 4c). The transition from facies IIA to facies IIB is gradational. Similar to facies IIA, facies IIB is also finely laminated and includes a few, sparse thin beds of khaki-coloured sandstone (facies IIC; Fig. 4c). These thin sandstone beds (facies IIC) are up to 7 cm thick, internally massive, have sharp bases and tabular in geometry. Their tops are planar, without any evidence of later reworking. Facies IIB is overlain by the coarse-grained siliciclastic Barakar Formation.

3.b.1. Interpretation

The basal fossiliferous ~50 cm of Facies Association II was presumably deposited in a palaeoenvironment similar to that of its counterpart at the base of Facies Association I. However, the absence of the isolated large unabraded granite boulders suggests a palaeogeographical position of Facies Association II relatively distant from the basement ridge which provided large, angular granite boulders. The occurrence of scattered and chaotic pebbles along with disarticulated fossil valves within facies IIA suggests that its origin was related to hyper-concentrated flows (Mulder & Alexander, 2001). Fossils were probably disarticulated during their transportation. The upwards transition of the black shale (facies IIA) into the grey shale (facies IIB) in Facies Association II indicates some overall improvement in basin-floor oxygenation. However, the well-laminated nature of facies IIB attests to the continuation of the same slow rate of sedimentation in a low-energy depositional setting as

before. The thin sheets of fine-grained sandstone (facies IIC) suggest periodic higher energy inputs into the basin. Internal massiveness, without any evidence of tractive currents or waves in the sandstone sheets, prompts their recognition as quasi-steady turbidites (Mulder & Alexander, 2001).

Figure 4. Facies Association II - (a) Marine fossil-bearing conglomerate bed (IIA); note that well-abraded granite pebbles are scattered along with the marine fossils. (b) Well-laminated fossil-free black shale (IIB). (c) Transition of facies IIB into grey shale facies (IIC) upwards, which is interspersed with thin sandstone sheets (white arrow); note that the top of the IIB facies is truncated by a sandstone body (demarcated by yellow dotted line)

3.c. Facies Association III

This facies association, having four sub-facies viz. black shale (facies IIIA), conglomerate (facies IIIB), grey shale (facies IIIC) and tabular sandstone (facies IIID), is well exposed at a location approximately 1.2 km to the NE from outcrops of Facies Associations I and II described above (Fig. 2). Similar to Facies Association II, black shale and rounded pebbles are also present, although fossils are conspicuously absent. In addition, black shale and pebbles are present in different arrangements as they now occur as alternating beds. Facies IIIA (Fig. 5a) and facies IIIB (Fig. 5b) beds have mean thicknesses of approximately 28 and 45 cm, respectively. Facies IIIB contains pebbles of similar composition to the previous facies association, although they are less than 4.5 cm long and have a black mud matrix. Pebbles show reverse grading. The pebble beds are tabular and sharp, and the vertical distance between successive beds is

approximately 50 cm. None of these beds bears any current structure. The shale-conglomerate alternation extends upwards approximately 3 m from the base of the section. Above, facies IIIA grades upwards into facies IIIC. The latter is similar to facies IIB and is also overlain by the Barakar Formation. It is sparingly interspersed with khaki-coloured sandstone bodies (facies IIID; Fig. 5c). The beds are tabular and massive, but thicker (~50 cm) than facies IIC. A few pebbles, approximately 5 cm long, may be dispersed within them.

Figure 5. Facies Association III - (a) Repeated alternations between black shale (IIIA) and conglomerate (IIIB). Note that the lower contact between IIIA and IIIB is sharp compared to the upper contact. (b) Matrix-supported conglomerate of facies IIIB. (c) Massive pebble-bearing sandstone (III C) showing imbrication at the lower part of the bed

3.c.1. Interpretation

In Facies Association III, the textural contrast in sediment is most remarkable. The black shale (facies IIIA) was deposited, as in other associations, in a calm and quiet basinal setting. The pebbles in the associated muddy conglomerates (facies IIIB) were likely delivered by melting icebergs and/or cohesive/hyperconcentrated flow or by both (comparison between these processes are discussed in Section 4). Neither a glacial nor density flow origin for the conglomerates necessitates any change in basin palaeogeography for the deposition of alternating shale and matrix-rich conglomerate beds. The grey shale (facies IIIC) at the top of Facies Association III may indicate relative improvement in water circulation during the deglaciation period within an otherwise restricted interior sea bottom. When the monotony of the grey shale (facies IIIC) lithology is interrupted by the appearance of the tabular sandstone facies (facies IIID), a sudden enhancement of depositional energy becomes imperative. There is no evidence for the action of tractive currents or waves in sand deposition. In contrast, the massiveness of the sandstone suggests instantaneous deposition, most likely from a sandy density flow.

3.d. Facies Association IV

Moving further NNE, approximately 1 km from outcrops of Facies Association III described above, are outcrops exhibiting Facies Association IV, comprising two sub-facies viz. grey shale (facies IVA; Fig. 6a) and lenticular sandstone bodies (facies IVB; Fig. 6b) which rests directly on the granitic basement (Fig. 2). The sandstone lenses (facies IVB; Fig. 6b) are present as channel forms with concave-up bases and flat tops (Fig. 6b) within the grey shale (facies IVA). Their infillings are coarser-grained and distinctly more poorly sorted than the sandstone beds of the other associations. The channel fills are thoroughly cross-stratified, and their maximum width and depth are 70 and 55 cm, respectively.

3.d.1. Interpretation

The gradational vertical contact with the marine black shale in Facies Associations II and III also testifies to the marine origin of the grey shale. Facies IVA rests directly on the granitic basement at the northern/landward flank of the interior sea (Fig. 2), implying that sea also onlapped the landward flank. If the vertical colour change from black to grey in the shale of Facies Associations II and III reflects the enhancement of water circulation, it most likely relates to the deglaciation event that affected the depositional site. This contention is strongly supported by the fact that the grey shale, irrespective of facies association, hardly ever contains any pebbles that can be identified as a dropstone. Facies IVB, because of its lenticular body geometry, sandy lithology, very poor grain sorting and internal current structures, can readily be attributed to a river entering the interior sea (Walker & Mossa, 1982; Mėžinė *et al.* 2019). Their channel-like geometry corroborates this contention.

Figure 6. Facies Association IV - (a) Grey shale (IVA) facies locally intervened y lenticular sandstone body (IVB). (b) Sandstone body (IVB) has a concave base and is internally characterized by cross-stratification.

4. Discussion

4.a. Glacial vs. density flow origin of the deposits

The map of the global distribution of ice sheets during the Late Palaeozoic glaciation by Montañez (2022) includes the present study area. The most convincing glacial feature is striated/boulder pavement, which could not be identified within the outcrop limits ñat Manendragarh, but has been documented from the Giridih and Satpura basins close to the present study area (Fig. 7). Varshney and Bhattacharya (2023) reported several signatures of deposition by melting glaciers near the ice grounding line at Manendragarh. In this section, pebbles belonging to conglomerates of different facies associations are considered to ascertain the mode/s of delivery of the pebbles to the depositional sites whether by glacier or by density flow. This account scrutinizes the general fabric in pebbly beds, the nature of their distribution and orientation of pebbles and the nature of bed contacts. The following are the features.

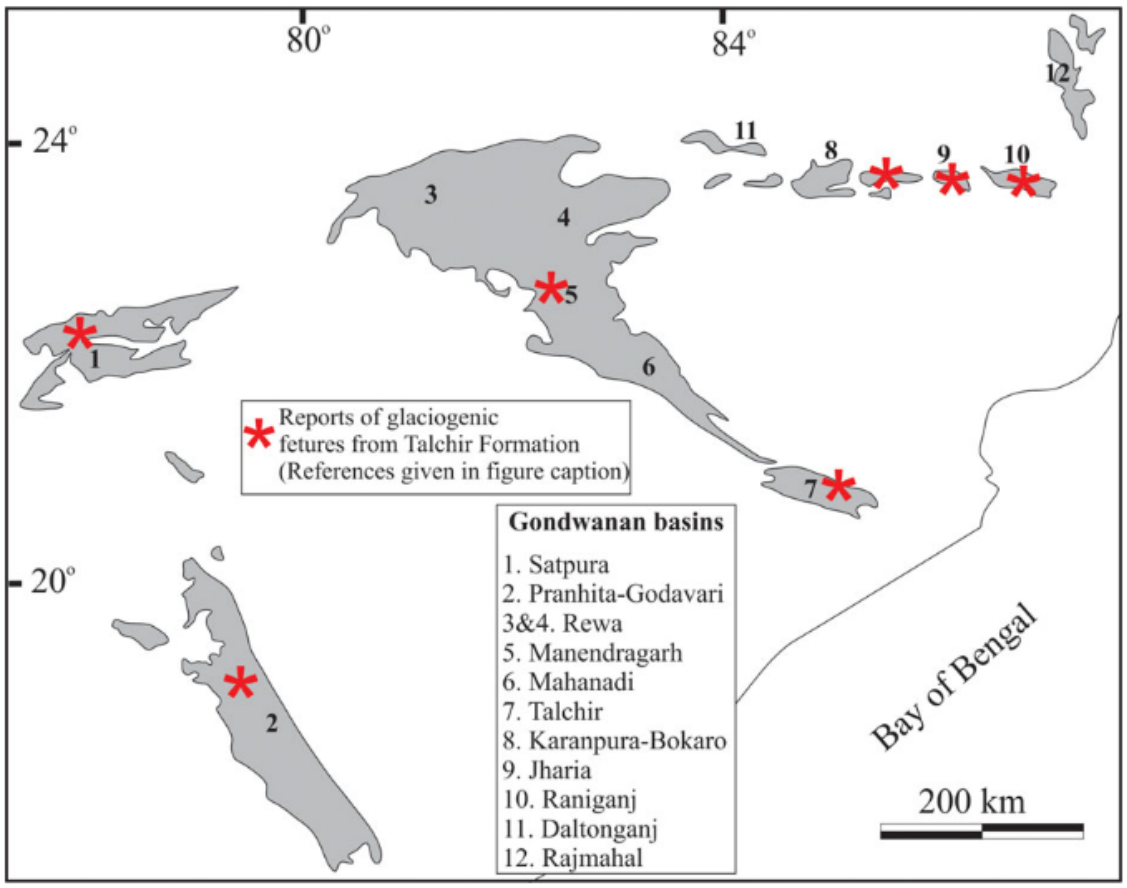

Figure 7. Map showing distribution of different Gondwanan basins of Peninsular India. Red coloured asterisks show the reports of glaciogenic deposits from Talchir Formation in and around the present study area by Smith (1963a); Sen (1991); Bose et al. (1992); Dasgupta (2006); Chakraborty and Ghosh (2008); Bhattacharya and Bhattacharya (2015); Varshney and Bhattacharya (2023).

4.a.1. Pebbles in hydrodynamic disequilibrium

In the pebble-bearing black shale (facies IIA) at the base of the Facies Association II and in some of the conglomerate beds (facies IIIB) in Facies Association III, pebbles are found to be significantly larger in vertical dimension than the thickness of laminae within the shales that host them (Fig. 8a–c). The pebbles are up to 8.5 cm long, and some isolated pebbles are in an upright position, while the lamina-thickness around them is on the mm scale (Fig. 8a). The pebbles are also faceted (Fig. 8d). They can be deposited from a hyperconcentrated flow with muddy matrix generated from a melting glacier near the ice grounding line (Varshney & Bhattacharya, 2023). Such pebbles in finely laminated shale can alternatively be volcanic bombs dropped from the air. However, no contemporary volcanic event has thus far been reported from nearby areas. Dropping from a floating iceberg on the water surface appears to be the most reasonable option. It appears that these pebbles must have been subjected to prolonged abrasion and attrition after being picked up by a glacier.

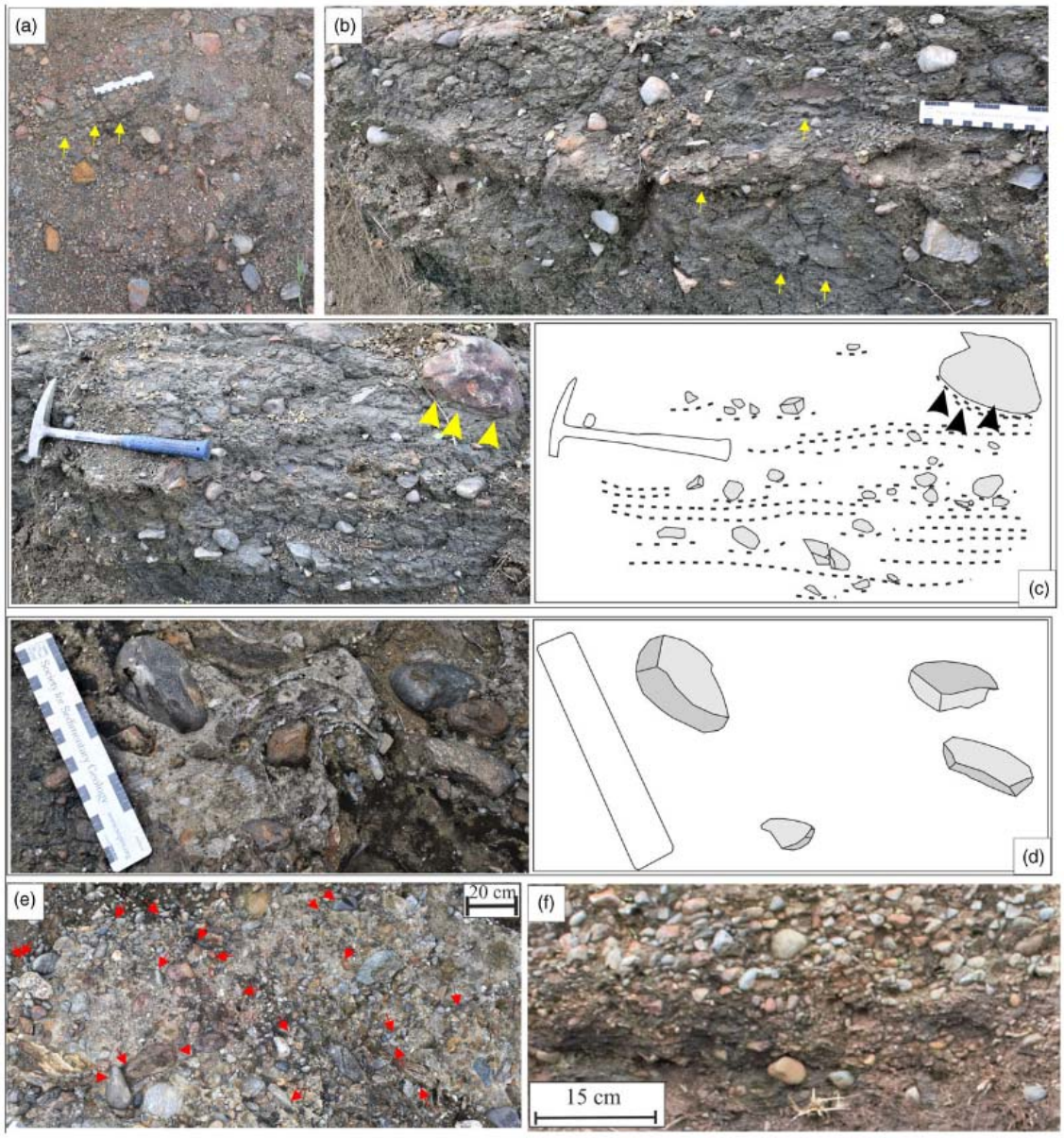

Figure 8. (a) Oversized pebbles present in upright position within the shale (IA); finer laminations (yellow arrows) are preserved within the shale (IA). (b) Pebbles in hydrodynamically disequilibrium conditions with respect to shale (IA); note that fine laminations (yellow arrows) are preserved within shale. (c) Field photo and a hand sketch show laminae within the shale are downwarped around the bottoms of the granite block. (d) Ill-faceted basement pebbles within the conglomerate. (e) Bullet-shaped pebbles pointing towards glacial abrasion. (f) Reverse-graded and clast-supported conglomerate with a sharp base, suggesting deposition from mass flow with strong shear at its base.

4.a.2. Bottom wrapping

Under some similarly well-abraded and isolated pebbles in black shale (facies IIA) in Facies Association II, laminae wrap around their bottoms (Fig. 8c). Apparently, the laminae were deformed under the impact created by the pebbles falling from above, possibly from floating icebergs. Alternatively, as pointed out earlier, the pebbles could also be volcanic bombs, had there been evidence of proximal volcanic eruption.

4.a.3. Indistinct base of conglomerate beds

In Facies Association III, it was mentioned that the upwards transition from diamictite (facies IIIB) to shale (facies IIIA) is always sharp, despite minor irregularities at the contact. However, the reverse transition is often indistinct because of the occurrence of some detached pebbles beneath the base of the conglomerate beds (Fig. 5a, dashed line). These pebbles are in no way in hydrodynamic equilibrium with the shale around them. They are thus interpreted to have sunk into the underlying mud and are possibly dropstones.

4.a.4. Faceted and bullet pebbles

As a glacier moves, pebbles held tightly at its base are rubbed against the rocky surface and consequently, those surfaces become flattened, polished and striated (Atkins, 2003, 2004). In the process, ice thawing may turn the pebble on its other side. As soon as thawing occurs, the friction, however, disappears, and the ice immediately reforms, temporarily preventing further rotation of the pebble. A new face of the pebble starts to flatten. Therefore, facets, particularly multiple facets on pebbles, are considered diagnostic of their glacial origin (Fig. 7d) and have been recorded from the conglomerate beds (facies IIIB) at different levels within Facies Association III. Apart from faceted pebbles, bullet-shaped pebbles (Fig. 8e) are another indicator of glacier abrasion (Krüger, 1984). It is, however, possible that faceted pebbles generated on land due to glacial abrasion could have been redeposited within the interior sea.

4.a.5. Imbricated pebbles

The rare sandstone beds (facies IIID) in Facies Association III are sharp-based and generally appear massive. Locally, they contain some pebbles that tend to concentrate in the lower part of the beds, affecting coarse-tail grading (Fig. 4c; Nemec *et al.* 1980; Schlunegger & Garefalakis, 2018). In certain instances, the pebbles are elongated and imbricated along their long axes (Fig. 5c). The coarse-tail grading suggests the concentrated flow of sand and pebbles together, along with the entrapped fluid. The long-axis imbrication of the pebbles further suggests that the flows had been internally sheared (Bose & Sarkar, 1991). Genetically, the massive fine-grained sandstone beds in Facies Association III are thus considered to be transitional between products of concentrated density flow and quasi-steady turbidity current (Mulder & Alexander, 2001).

4.a.6. Sharp-based reverse-graded conglomerate

The hyperconcentrated/concentrated flow beds are always sharp-based, whether they are clast-supported or (unlaminated) matrix-supported. In glacier-imprinted formations, they are bound to create controversy regarding their origin. Grading, (whether normal or reverse) favours concentrated density flow interpretation. The reverse grading illustrated in Fig. 8f in a clast-supported conglomerate (facies IIIB) suggests deposition from a concentrated density flow with strong shear at its base. The vertical component of the dispersive pressure generated as a reaction to the basal shear presumably tended to push the clasts upwards; the larger clasts were pushed farther from the base. It can be conceived that a clast settled only

when its settling velocity exceeded the dispersive pressure. The mechanism would suggest that the flow slowed from the top downwards.

4.b. Depositional conditions

An overall interpretation of the facies associations within the Talchir Formation in Manendragarh suggests its deposition within an interior sea. The spatial variation in the characteristics of the facies associations, notwithstanding the predominance of shale, indicates that the basin had its seaward margin on the south and the landward margin to the north. The basin formed when the sea transgressed over a basement ridge, and the large fragmented blocks recorded in the outcrops (Fig. 3a, b) may reflect the proximity and steepness of this ridge. Glacial dropstones accumulated in the interior of the basin, with faceted and bullet pebble deposits (Fig. 8c–e) and density flows (Figs. 5c, 8f), were induced by glacial meltwaters. Fielding *et al.* (2008b) viewed the Permian glaciation as a four-phase event. Shah and Shastry (1975) and Dickins and Shah (1979), based on palaeontological evidence, correlated the Manendragarh glacier to the late stage of the first phase (P1). The initial transgression mentioned above could be the result of the first phase (P1) of deglaciation. The marine invertebrate fauna thrived in the lower part of Facies Associations I and II but failed to colonize the landward part of the interior sea (within Facies Association III and IV). It is possible that the marine organisms that invaded at the early stage of basin evolution were opportunistic and tried to colonize this newly created niche. Nonetheless, their colony remained confined to the vicinity of the seaward margin of the basin and only for a relatively short period. On the other hand, glacial dropstones as well as pebbly hyperconcentrated/concentrated flows and turbidites became important in the interior part of the basin. In the final phase of deglaciation, the shale turned grey and onlapped over the landward basin margin. Sandy turbidites (facies IIID) driven by glacial meltwater interrupted the grey shale (facies IIIC) sequence building periodically. The meltwater channel mouths interrupted the grey shale close to the land margin. The repeated alternation between shale and diamictite in Facies Association III, however, appears to be the product of shorter-scale glacial-interglacial transitions (Yang *et al.* 2018). There is a consensus that the Gondwana glaciation was most intense during the first (P1) and second (P2) phases and had a low CO 2 (1.0 X –1.5 X Present day Atmospheric Level) (Isbell *et al.* 2003; Montañez *et al.* 2007). In such a setting, only a slight change in solar radiation could have caused the observed switchovers between glacial and interglacial regimes (Riechers *et al.* 2022).

Through time, the black shale graded upwards to the grey shale, but a lack of preserved current structures points to the fact that the interior sea still remained a calm water basin. The postglacial grey shale, devoid of any dropstones, is interbedded with sandy turbidites that were triggered by glacial meltwater fluxes (Horan *et al.* 2019).

5. Conclusions

Marine fossil-bearing black shale resting directly on top of the granite basement indicates a rapid marine transgression in Manendragarh at the end of the P1 phase of Late Palaeozoic glaciation. The presence of isolated and sharply angular granite blocks within the black shale suggests deposition in an interior sea that was generated behind a steep basement ridge. The

ice sheets did not extend beyond the deepest part of the interior sea, and the biotic colony could only invade the fringes of the interior sea, where it flourished for limited periods. Hence, during intermediate deglaciation phases, the seaward edge of the lagoon experienced the accumulation of thin calcarenite layers, while in central region of the interior sea, accumulation of black shale alternated with pebbly dropstones and hyperconcentrated flows. In the final deglaciation, grey shale deposition became dominant and was interrupted by rare sandy gravity flows and hyperconcentrated flows triggered by glacial meltwater fluxes. At the landward margin of the interior sea, feeder channels of these sandy gravity flows were locally incised and preserved. Dominance of sandy gravity flows and hyperconcentrated flows towards the upper part of the studied succession indicate decreasing influence of glaciogenic processes due to climatic changes during the Late Palaeozoic of northern Gondwana.

Acknowledgements

The authors acknowledge Emese Bordy (the Executive Editor), Pierre Dietrich, A.J. Tom Van Loon and the two anonymous reviewers whose comments helped to improve the manuscript. AC, SM and SKP acknowledge the Director of BSIP, Lucknow, for giving this opportunity for fieldwork in the studied area. AC and SM are indebted to Prof. Pradip K. Bose for advising all along and reviewing a previous version of the manuscript as well as suggesting its improvement. AC, SM and SKP acknowledge the Chattisgarh State Biodiversity Board and Forest Department for their hospitality and cooperation throughout the fieldwork and the Geological Survey of India, Raipur, for providing necessary help during the fieldwork. They also acknowledge BSIP, Lucknow, for the infrastructure (Publication No. 62/2021-22).

Competing interests

The authors declare no conflict of interest.

References

Acharya S (2018) Tectonic Setting and Gondwana Basin Architecture in the Indian Shield: Elsevier, p. 153.

Atkins CB (2003) Characteristics of Striae and Clasts in Glacial and Non-Glacial Environments. Wellington, New Zealand: Victoria University of Wellington, p. 321.

Atkins CB (2004) Photographic Atlas of Striations from Selected Glacial and Non-Glacial Environments. Antarctic Data Series No 28. A Publication of the Antarctic Research Centre. Wellington: Victoria University of Wellington. pp. 1–45.

Banerjee S, Ghosh P, Nagendra R, Bhattacharya B, Desai B and Srivastava AK (2020) Marine and fluvial sedimentation including erosion and sediment flux in Peninsular Indian Phanerozoic Basins. Proceedings of Indian National Science Academy 86, 351–63.

Beard JA, Ivany LC and Runnegar B (2015) Gradients in seasonality and seawater oxygen isotopic composition along the early Permian Gondwanan coast, SE Australia. Earth and Planetary Science Letters 425, 219–31.

Bharti S and Chakraborty S (2014) First record of palynoflora from the early Permian marine sequence in the Talchir formation of Tawa Valley of Satpura Basin, Madhya Pradesh, India. Indian Journal of Geosciences 68, 31–6.

Bhatia SB and Saxena IP (1957) Occurrence of the genus hyperammina in the marine Permo-Carboniferous bed at Umaria, Central India. Contribution to Cushman Foundation for Foraminiferal Research 8, 146–8.

Bhatia SB and Singh SK (1959) Carbonaceous (Uralian) foraminifera from Manendragarh, Central India. Micropaleontology 5, 127–34.

Bhattacharya B (2013) Sedimentary cycles related to the late Palaeozoic cold-warm climate change, Talchir formation, Talchir Basin, India. Earth Resources 1, 12–25.

Bhattacharya B and Bhattacharya HN (2012) Implications of mud-clast conglomerates within late Palaeozoic Talchir glaciomarine succession, Talchir Basin, India. Indian Journal of Geosciences 66, 69–78.

Bhattacharya HN and Bhattacharya B (2006) A Permo-Carboniferous tide-storm interactive system: Talchir formation, Raniganj Basin, India. Journal of Asian Earth Sciences 27, 303–11.

Bhattacharya HN and Bhattacharya B (2010) Soft-sediment deformation structures from an ice-marginal storm-tide interactive system, PermoCarboniferous Talchir Formation, Talchir Coalbasin, India. Sedimentary Geology 223, 380–9.

Bhattacharya HN and Bhattacharya B (2015) Lithofacies architecture and Palaeogeography of the Late Paleozoic glaciomarine Talchir Formation, Raniganj Basin, India. Journal of Palaeogeography 4, 269–283.

Bhattacharya HN, Bhattacharya B, Chakraborty I and Chakraborty A (2004) Sole marks in storm event beds in the Permo-Carboniferous Talchir Formation, Raniganj Basin, India. Sedimentary Geology 166, 209–22.

Bhattacharya HN, Chakraborty A and Bhattacharya B (2005) Significance of transition between Talchir formation and Karharbari formation in lower Gondwana Basin evolution—a study in West Bokaro Coal Basin, Jharkhand, India. Journal of Earth System Science 114, 275–86.

Blakey RC (2008) Gondwana paleogeography from assembly to breakup—a 500 m.y. odyssey. In Resolving the Late Paleozoic Ice Age in Time and Space (eds CR Fielding, TD Frank and JL Isbell), p. 441. Boulder, CO: Geological Society of America Special Paper.

Bose PK, Mazumder R and Sarkar S (1997) Tidal sandwaves and related storm deposits in the transgressive Protoproterozoic Chaibasa Formation, India. Precambrian Research 84, 63–81.

Bose PK, Mukhopadhyay G and Bhattacharyya HN (1992) Glaciogenic coarse clastics in a Permo-Carboniferous bedrock trough in India: a sedimentary model. Sedimentary Geology 76, 79–97.

Bose PK and Sarkar S (1991) Basinal autoclastic mass flow regime in the Precambrian Chanda Limestone formation, Adilabad, India. Sedimentary Geology 73, 299–315.

Buggisch W, Wang X, Alekseev AS and Joachimski MM (2011) Carboniferous-Permian carbon isotope stratigraphy of successions from China (Yangtze platform), USA (Kansas) and Russia (Moscow Basin and Urals). Palaeogeography Palaeoclimatology Palaeoecology 301, 18–38.

Caputo MV, Goncalves de Melo JH, Streel M and Isbell JL (2008) Late Devonian and early Carboniferous glacial records of South America. In Resolving the Late Paleozoic Ice Age in Time and Space (eds CR Fielding, TD Frank and JL Isbell), p. 441. Boulder, CO: Geological Society of America Special Paper.

Casshyap SM and Qidwai HA (1974) Glacial sedimentation of late Palaeozoic Talchir diamictite, Pench valley coalfield, central India. Geological Society of American Bulletin 85, 749–60.

Casshyap SM and Tewari RC (1982) Facies analysis and palaeo-geographic implications of a Late Palaeozoic glacial outwash deposit. Bihar, India. Journal of Sedimentary Petrology 52, 1243–56.

Casshyap SM and Tewari RC (1984) Fluvial models of the Lower Permian Gondwana coal measures of Son- Mahanadi and Koel-Damodar basins. In: Sedimentology of Coal and Coal Bearing Strata (eds RA Rahmani and RM Flores), 7, pp. 121–147: Special Publication International Association of Sedimentogy.

Chakrabarty A (1993) Marine influence during Talchir deposition, Giridih Basin, Bihar. Indian Journal of Geology 65, 290–2.

Chakraborty C and Ghosh SK (2008) Pattern of sedimentation during the Late Paleozoic, Gondwanaland glaciation: an example from the Talchir Formation, Satpura Gondwana basin, central India. Journal of Earth System Science 117, 499–519.

Chandra SK (1996) Marine signature in the Gondwana of Peninsular India and Permian palaeogeography. In: Proceedings of IXth International Gondwana Symposium (eds PKS Guha, *et al.*), 1, pp. 529–38. Hyderabad: Geological Survey of India.

Chiarle M, Iannotti S, Mortara G and Deline P (2007) Recent debris flow occurrences associated with glaciers in the Alps. Global and Planetary Change 56, 123–36.

Christ RD and Wernil Sr RL (2014) Chapter 2–The Ocean Environment. The ROV Manual, 2nd edn, pp. 21–52. Butterworth-Heinemann.

Cisterna AG, Sterrn AF, Shi GR, Halpern K and Balseiro D (2019) Brachiopod assemblages of the eurydesma fauna in glacialdeglacial sequences from Argentina and Australia. Rivista Italiana di Paleontologia e Stratigrafia 125, 805–26.

Das SN and Sen DP (1980) Depositional history of Permo-Carboniferous tillites and associated sediments in West Bokaro Gondwana basin, Bihar. Journal of the Geological Society of India 21, 30–8.

Dasgupta P (2006) Facies characteristics of Talchir formation, Jharia Basin, India: implications for initiation of Gondwana sedimentation. Sedimentary Geology 185, 59–78.

Dasgupta S (2021) A review of stratigraphy, depositional setting and Paleoclimate of the Mesozoic Basins of India. In Mesozoic Stratigraphy of India: A Multi-Proxy Approach (eds S Banerjee and S Sarkar), pp. 1–11. Cham: Springer Nature Switzerland AG, SES Series.

Dickins JM (1957) Lower Permian pelecypods and gastropods from the Carnavon basin, western Australia. Bureau of Mineral Resources, Geology and Geophysics Bulletin 41, 1–74.

Dickins JM and Shah SC (1979) Correlation of the Permian marine sequences of India and Western Australia. In Proceedings IV Gondwana Symposium (Calcutta, India), vol. 2. India: Hindusthan Publishing Corporation, pp. 387–408.

Dietrich P, Franchi F, Setlhabi L, Prevec R and Bamford M (2019) The nonglacial diamicite of Toutswemogala Hill (lower Karoo Supergroup, central Botswana): implications on the extent of the late Paleozoic ice age in the Kalahari-Karoo Basin. Journal of Sedimentary Research 89, 875–89.

Dutta AK (1957) Occurrence of Eurydesma horizon near Manendragarh, M.P. Science Culture 26, 569–70.

Eyles N and McCabe AM (1989) The late Devensian (<22000YBP) Irish Sea Basin: the sedimentary record of a collapsed ice sheet margin. Quaternary Science Review 8, 307–51.

Fielding CR, Bann KL, Maceachern JA, Tyes SC and Jones BG (2006) Cyclicity in the nearshore marine to coastal, Lower Permian, Pebbley Beach Formation, southern Sydney Basin, Australia: a record of relative sea-level fluctuations at the close of the Late Palaeozoic Gondwanan ice age. Sedimentology 53, 435–63.

Fielding CR, Frank TD, Birgenheier LP, Rygel MC, Jones AT and Roberts J (2008a) Stratigraphic imprint of the Late Palaeozoic Ice Age in eastern Australia: a record of alternating glacial and non-glacial climate regime. Journal of Geological Society of London 165, 129–40.

Fielding CR, Frank TD, Birgenheier LP, Rygel MC, Jones AT and Roberts J. (2008d) Stratigraphic record and facies associations of the late Paleozoic ice age in eastern Australia (New SouthWales and Queensland). In Resolving the Late Paleozoic Ice Age in Time and Space (eds CR Fielding, TD Frank and JL Isbell), p. 441. Boulder, CO: Geological Society of America Special Paper.

Fielding CR, Frank TD and Birgenheir LP (2022) A revised, late Palaeozoic glacial time-space framework for eastern Australia, and comparison with other regions and events. Earth Science Reviews 236, 104263.

Fielding CR, Frank TD and Isbell JL (2008c) The late Paleozoic ice age—a review of current understanding and synthesis of global climate patterns. Geological Society of America Special Paper 441, 343–54.

Fielding CR, Frank TD and Isbell JL (eds) (2008b) Resolving the late Paleozoic Ice Age in time and space. Geological Society of America Special Publication 441, 1–354.

Fielding CR, Frank TD, Isbell JL, Henry LC and Domack EW (2010) Stratigraphic signature of the late Paleozoic Ice Age in the Parmeener Supergroup of Tasmania, SE Australia, and inter-regional comparisons. Palaeogeography Palaeoclimatology Palaeoecology 298, 79–90.

Frakes LA and Francis JE (1988) A guide to Phanerozoic cold polar climates from high-latitude ice-rafting in the Cretaceous. Nature 333, 547–49.

Frakes LA, Francis JE and Syktus JI (1992) Climate Modes of the Phanerozoic. Cambridge, UK: Cambridge University Press.

Frakes LA, Kemp EM and Crowell JC (1975) Late Paleozoic glaciation: part VI, Asia. Geological Society of American Bulletin 86, 454–64.

Frank TD, Shultis AI and Fielding CR (2015) Acme and demise of the late Palaeozoic ice age: a view from the southeastern margin of Gondwana. Palaeogeography Palaeoclimatology Palaeoecology 418, 176–92.

Garbelli C, Shen SZ, Immenhauser A, Brand U, Buhl D, Wang WQ, Zhang H and Shi GR (2019) Timing of early and middle Permian deglaciation of the southern hemisphere: Brachiopod-based 87Sr/86Sr calibration. Earth and Planetary Science Letters 516, 122–35.

Ghosh S (1954) Discovery of a new locality of marine Gondwana formation near Manendragarh in Madhya Pradesh. Science Culture 19, 620.

Ghosh S (2003) First record of marine Bivalves from the Talchir Formation of the Satpura Gondwana Basin, India: Palaeobiogeographic implications. Gondwana Research 6, 312–20.

Griffis N, Montañez I, Mundil R, Heron DL, Dietrich P, Kettler C, Linol B, Mottin T, Vesely F, Iannuzzi R, Huyskens M and Yin QZ (2021) High-latitude ice and climate control on sediment supply across SW Gondwana during the Late Carboniferous and early Permian. Geological Society of America Bulletin 133, 2113–24.

Horan K, Stone P and Crowhurst SJ (2019) Sedimentary record of Early Permian deglaciation in southern Gondwana from the Falkland Islands. In Glaciated Margins: The Sedimentary and Geophysical Archive (eds DP Le Heron, KA Hogan, ER Phillips, M Huuse, ME Busfield and AGC Graham), 475, pp. 131–147. London: Geological Society of London Special Publications.

Hyde WT, Crowley TJ, Tarasov L and Peltier WR (1999) The Pangean ice age: studies with a coupled climate-ice sheet model. Climate Dynamics 15, 619–29.

Isbell JL, Henry LC, Gulbranson EL, Limarino CO, Fraiser ML, Koch ZJ, Cicioli PL and Dineen AA (2012) Glacial paradoxes during the late Paleozoic ice age: evaluating the equilibrium line altitude as a control on glaciation. Gondwana Research 22, 1–19.

Isbell JL, Miller MF, Wolfe KL and Lenaker PA (2003) Timing of late Paleozoic glaciation in Gondwana: Was glaciation responsible for the development of Northern Hemisphere cyclothems? Geological Society of America Special Paper 370, 5–24.

Isbell JL, Taboada AC, Koch ZJ, Limarino CO, Frasier ML, Pagani MA, Gulbranson EL, Ciccioli PL and Dineen AA (2011) Emerging polar view of the late Paleozoic ice age as interpreted from

deep-water distal, glacimarine deposits in the Tepuel-Genoa Basin, Patagonia, Argentina. In Programme & Abstracts, XVII International Congress on the Carboniferous and Permian (eds E Hakansson and J Trotter), p. 74. Perth: Geological Survey of Western Australia.

Ivany LC and Runnegar B (2010) Early Permian seasonality from bivalve δ18O and implications for the oxygen isotopic composition of seawater. Geology 38, 1027–30.

James NP, Frank TD and Fielding CR (2009) Carbonate sedimentation in a Permian highlatitude, subpolar depositional realm. Queensland, Australia. Journal of Sedimentary Research 79, 125–43.

Krüger J (1984) Clasts with stoss-lee form in lodgement tills: a discussion. Journal of Glaciology 30, 241–3.

Le Heron DP, Kettler C, Wawra A, Schöpfer M and Grasemann B (2022) The sedimentological death mask of a dying glacier. The Depositional Record 8, 992–1007.

Maejima W, Das R, Pandya KL and Hayashi M (2004) Deglacial control on sedimentation and basin evolution of Permo-Carboniferous Talchir Formation, Talchir Gondwana Basin, Orissa, India. Gondwana Research 72, 339–52.

Mėžinė J, Ferrarin C, Vaiciute D, Idzelyt˙e R, Zemlys P and Umgiesser G (2019) Sediment transport mechanisms in a lagoon with high river discharge and sediment loading. Water 11, 1–24.

Mondal S, Mukherjee D, Iangrai B, Roy A and Sinha S (2021) Early Permian macroinvertebrate assemblages from the Siang and Subansiri districts, Arunachal Pradesh: implications on the regional stratigraphy, palaeoenvironment, palaeoecology, and palaeobiogeography. Journal of Earth System Science 130, 1–23.

Montañez IP (2022) Current synthesis of the penultimate icehouse and its imprint on the Upper Devonian through Permian stratigraphic record. In The Carboniferous Timescale (eds SG Lucas, JW Schneider, X Wang and S Nikolaeva), 512, pp. 213–45. London: Geological Society, Special Publications.

Montañez IP and Poulson CJ (2013) The late Paleozoic Ice Age: an evolving paradigm. Annual. Review of Earth Planetary Science 41, 629–56.

Montañez IP, Tabor NJ, Niemeier D, DiMichele WA, Frank TD, Fielding CR, Isbell JL, Birgenheier LP and Rygel MC (2007) CO2-forced climate and vegetation instability during late Paleozoic Deglaciation. Science 315, 87–91.

Mukherjee D, Ray S, Chandra S, Pal S and Bandopadhyay S (2012) Upper Gondwana succession of the Rewa Basin, India: understanding the interrelationship of Lithologic and stratigraphic variables. Journal of Geological Society of India 79, 563–75.

Mukhopadhyay G and Bhattacharya HN (1994) Facies analysis of Talchir sediments (permo-carboniferous), Dudhi Nala, Bihar, India–a Glaciomarine Model. In IXth International Gondwana Symposium, New Delhi: Oxford and IBH Publication, 2, pp. 737–53.

Mukhopadhyay G, Mukhopadhyay SK, Roy Chowdhury M and Parui PK (2010). Stratigraphic correlation between different Gondwana Basins of India. Journal of Geological Society of India 76, 251–66.

Mulder T and Alexander J (2001) The physical character of subaqueous sedimentary density flows and their deposits. Sedimentology 48, 269–99.

Nemec W, Porębski SJ and Steel RJ (1980) Texture and structure of resedimented conglomerates: examples from Książ Formation (Famennian—Tournaisian), southwestern Poland. Sedimentology 27, 519–38.

Pascoe EH (1968) A Manual of Geology of India and Burma. vol. 2. Calcutta: Government of India Press.

Pérez Loinaze VS, Limarino CO and Cesari SN (2010) Glacial events in Carboniferous sequences from Paganzo and Rio Blanco Basins (Northwest Argentina): palynology and depositional setting. Geologica Acta 8, 399–418.

Posamentier HW and Walker RG (eds.) (2006). Facies models revisited. SEPM Special Publication 84. p. 521.

Ram-Awatar, Meherotra RC, Srivastava R, Yadav KC and Gautam S (2013) Further contributions to the palynological studies showing marine incursion in the Talchir formation, Manendragarh, Koriya District, Chhattisgarh. Science and Technology Journal 1, 3–7.

Reed FRC (1928) A Permo-Carboniferous marine fauna from Umaria Coalfield. Journal of Geological Society of India 60, 367–98.

Reed FRC (1932) New fossils from the agglomeratic slate of Kashmir. Memoirs of Geological Survey. Palaeontologia. India, New Series 20, 1–79.

Riechers K, Mitsui T, Boers N and Ghil M (2022) Orbital insolation variations, intrinsic climate variability, and Quaternary glaciations. Climate of the Past 18(4), 863–893.

Rogala B, James NP and Reid CM (2007) Deposition of polar carbonates during interglacial highstands on an Early Permian shelf, Tasmania. Journal of Sedimentary Research 77, 587–606.

Sahni MR and Dutt DK (1959) Argentine and Australian affinities in a Lower Permian fauna from Manendragarh, central India. Records of the Geological Survey of India 87, 655–70.

Schlunegger F and Garefalakis P (2018) Clast imbrication in coarse-grained mountain streams and stratigraphic archives as indicator of deposition in upper flow regime conditions. Earth Surface Dynamics 6, 743–61.

Sen DP (1977) Striated pavement to the east of Karmatanr, Bihar, India. Journal of Geological Society of India 18, 512–4.

Sen DP (1991) Sedimentation patterns of the Talchir group in the Giridih Gondwana basin, India: a case of multiple glacial advance and retreat. Palaeogeography Palaeoclimatology Palaeoecology 86, 339–52.

Shah SC and Shastry MVA (1975) Significance of early Permian fauna of Peninsular India. In Gondwana Geology. 3rd Gondwana Symposium (ed KSW Campbell), pp. 391–5. Canberra, Australia: Australian National University Press.

Shen SZ, Zhang H, Shi GR, Li WZ, Xie JF, Mu L and Fan JX (2013). Early Permian (Cisuralian) global brachiopod palaeobiogeography. Gondwana Research 24, 104–24.

Simoes MG, Neves JP, Taboadac AC, Pagani MA, Varejaoe FG and Assine ML (2020) Macroinvertebrates of the Capivari marine bed, late Paleozoic glacial Itarare Group, northeast Parana Basin, Brazil: Paleoenvironmental and paleogeographic implications. Journal of South American Earth Sciences 98, 102433.

Sinor KP (1923) Rewah state coalfields. Bulletin of Geological Department Rewah State 2, 73.

Smith AJ (1963a) Evidence for a Talchir (Lower Gondwana) glaciation: Striated pavement and Boulder bed at Irai, Central India. Journal of Sedimentary Petrology 33, 739–50.

Smith AJ (1963b) A striated pavement below the basal Gondwana sedimentation the Ajay river, Bihar, India. Nature 198, 880.

Stephenson MH, Angiolini L and Leng MJ (2007) The early Permian fossil record of Gondwana and its relationship to deglaciation: a review. In Deep-Time Perspectives on Climate Change: Marrying the Signal from Computer Models and Biological Proxies (eds M Williams, AM Haywood, FJ Gregory, DN Schmidt), vol. 2, pp. 1–60. London: The Micropalaeontological Society, Special Publications, Geological Society of London.

Taboada AC (2010) Mississippian–early Permian brachiopods from western Argentina: tools for middle- to high-latitude correlation, paleobiogeographic and paleoclimatic reconstruction. Palaeogeography Palaeoclimatology Palaeoecology 298, 152–75.

Taboada AC, Neves JP, Weinschutz LC, Pagani MA and Simoes MG (2016) Eurydesma–lyonia fauna (early permian) from the Itarare group, Parana Basin (Brazil): a paleobiogeographic W–E trans-gondwanan marine connection. Palaeogeography Palaeoclimatology Palaeoecology 449, 431–54.

Tiranti D and Deangeli C (2015) Modeling of debris flow depositional patterns according to the catchment and sediment source area characteristics. Frontiers of Earth Science 3, 1–14.

Tiwari BS (1958) Fossils from Madhya Pradesh. Science Culture 23, 655–6.

Varshney H and Bhattacharya B (2023) Implications of Late Palaeozoic postglacial marine transgressive-regressive (T-R) cycles recorded in the Talchir Formation, Son Valley Basin, peninsular India: a sequence stratigraphic paradigm. Geological Journal 58, 333–55.

Veevers JJ and Powell CM (1987) Late Paleozoic glacial episodes in Gondwanaland reflected in transgressive-regressive depositional sequences in Euramerica. Geological Society of American Bulletin 98, 475–87.

Veevers JJ and Tewari RC (1995) Gondwana master basin of Peninsular India between Tethys and the interior of the Gondwanaland Province of Pangea. Memoir Geological Society of America 187, 1–73.

Venkatachala BS and Tiwari RS (1987) Lower Gondwana marine incursions: periods and pathways. The Paleobotanist 36, 24–9.

Vesely FF, Rodrigues MCNL, da Rosa ELM, Amato JA, Trzaskos B, Isbell JL and Fedorchuk ND (2018) Recurrent emplacement of non-glacial diamictite during the late Paleozoic ice age. Geology 46, 615–618.

Walker HJ and Mossa J (1982) Effects of artificial structures on coastal lagoonal processes and forms. Oceanologica Acta Special issue (0399-1784), 191–198.

Wopfner H and Jin XC (2009) Pangea megasequences of Tethyan Gondwana-margin reflect global changes of climate and tectonism in Late Palaeozoic and Early Triassic times- a review. Palaeoworld 18, 169–92.

Yang B, Shi GR, Lee S and Luo M (2018) Co-occurrence patterns of ice-rafted dropstones and brachiopods in the Middle Permian Wandrawandian Siltstone of the southern Sydney Basin (southeastern Australia) and palaeoecological implications. Journal of the Geological Society Australia 175, 850–864.

Ziegler AM, Hulver ML and Rowley DB (1997) Permian world topography and climate. In Late Glacial and Postglacial Environmental Changes: Quarternary Carboniferous-Permian, and Proterozoic (ed IP Martini), pp. 111–46. Oxford, UK: Oxford University Press.